Chapter 4

On the Squeeze-film Characteristics between a Rotating Sphere and a Radially Rough Plate

Contents

4.1 Introduction

Squeeze-film behaviour arises when two lubricated surfaces approach each other with a normal velocity, known as squeeze velocity. Squeeze-film behaviour always have an attraction for researcher because of its appearance in many fields of real life, for example (a) in industry, it is observed in machine tools, gears, rolling elements, hydraulic systems, engines, clutch plates, etc. (b) in human body, it is observed in the study of skeletal joints as bio-lubrication. Due to this motivation many theoretical and experimental investigations were made on squeeze-film phenomenon by several investigators from different viewpoints. As reported by Gould [1], the study of squeeze-films was developed more rigorously by Reynolds [2]. The equations derived and integrated were applicable to the situation in which a Newtonian fluid of invariable properties was being slowly squeezed out of the space between two rigid, flat parallel plates with elliptical boundaries. Many configurations were investigated by Archibald [3] for the case when the surfaces remain parallel during the approach. Jackson [4] included both viscous and inertia effects in an investigation of the squeeze-film between plane discs. An excellent review of the work in squeeze-films up to 1965 has been given by Moore [5]. Christensen [6] has analyzed the elastohydrodynamic problem on normal approach of two spherical bodies. According to results, the effect of elastic deformation profoundly influences all aspects of motion when the separation of two surfaces becomes narrow enough. Gould [7] examined the same problem by considering the lubricant to be a function of pressure and temperature, and showed the effect of temperature on the characteristics of high-pressure squeeze-films. Conway and Lee [8] studied the squeeze-film characteristics between a sphere and a flat plate.They found

that the effect of increase in viscosity of the lubricant with pressure causes large increase of pressure near the central area as compared with the pressure obtained for isoviscous lubricant.The other authors worked in this direction from different viewpoints are given in   [9-11].

All above authors have studied various geometry of bearing surfaces on the assumption that the surfaces are perfectly smooth. However, in the production of bearings, presence of surface roughness pattern always exists up to certain extent. Several studies were made concerning the bearing design systems including roughness effect. It has been pointed out that load-carrying capacity, frictional force etc. can differ from their values for a smooth surface and this difference depends mainly on the amplitudes and wavelengths of the waves representing the rough surface. Burton [12] studied the effect of surface roughness on the load supporting characteristics of a lubricant film by postulating the sinusoidal variations in film thickness. Davies [13] used the saw tooth curve to study the effect of surface roughness on the generation of pressure between rough, fluid lubricated moving deformable surfaces. Tzeng and Saibel [14] made study of surface roughness effect on slider bearing lubrication using probability density function for random variable characterizing the surface roughness. Using stochastic method, Christensen [15] studied hydrodynamic lubrication of rough surfaces to analyze the effects of surface roughness on the squeeze-film lubrication between the curved circular plates. Tonder [16] made theoretical study of transition between surface distributed waviness and random roughness. Christensen and Tonder [17] studied hydrodynamic lubrication of rough journal bearings. Prakash and Christensen [18] used the stochastic theory to study the surface roughness effects on squeeze-film lubrication

between two rectangular plates. Prakash and Tiwari [19] studied effect of surface roughness on the characteristics of porous bearings using Christensen's stochastic theory. Andharia *et. al.* [20] studied the effect of surface roughness on the behaviour of a squeeze-film in a spherical bearing in transverse direction. Lin *et. al.* [21] have studied the effect of surface roughness on the oscillating squeeze-film behaviour of long partial bearings. Naduvinamani *et. al.* [22] studied the roughness effect on the squeeze-film formed by a sphere and a plate using couple-stress fluid. They showed that surface roughness effect considerably influences on squeeze-film characteristics. Bujurke *et. al.* [23] showed the effect of surface roughness on squeeze-film behaviour in porous circular discs using couple-stress fluid. They have shown that effect of couple-stress fluid and surface roughness is more pronounced as compared to classical one. More recently, Basti [24] discusses the effect of surface roughness and couple-stress fluid on squeeze-films formed between curved annular plates. It was shown that the circumferential roughness pattern on the curved annular plate results in more pressure buildup whereas performance of the squeeze-film suffers due to the radial roughness pattern for both concave and convex plates.

In recent years, many theoretical and experimental inventions are made on the bearing design system as well as on the lubricating substances in order to increase the efficiency of the bearing performances. One of the major revolutions in the direction of lubricating substances is an invention of ferrofluids. Ferrofluids (FFs) or Magnetic fluids (MFs) [25] are stable colloidal suspensions containing fine ferromagnetic particles dispersing in a liquid, called carrier liquid, in which a surfactant is added to generate a coating layer preventing the flocculation of the particles. When an external magnetic field

H is applied, FFs experience magnetic body force $(\mathbf{M} \bullet \nabla)\,\mathbf{H}$ which depends upon the magnetization vector **M** of ferromagnetic particles. Owing to these features, FFs are useful in many applications like in sensors, sealing devices, filtering apparatus, elastic damper, bearings, etc.[26- 30].

With the advent of FFs [25], many researchers have tried to find its applications as lubricant in bearing design system. Agrawal [31] studied effects of MF on a porous inclined slider bearing and found that the magnetization of the magnetic particles in the lubricant increases load-carrying capacity without affecting the friction on the moving slider. Chi *et. al.* [32] discuss new type of FF lubricated journal bearing consists of three pads. One of them is a deformable elastic pad. The theoretical analysis and experimental investigation shows that the performance of the bearing is much better than that of ordinary bearings. Moreover, the bearing operated without leakage and any feed system. Sinha *et. al.* [33] discuss about FF lubricated cylindrical rollers with cavitation. Recently, Uhlmann *et. al.* [34] discuss about application of MFs in tribotechnical systems. The rheological and tribological behaviour of MFs was investigated and compared with conventional lubricants between friction pairs under boundary conditions. Ahmad and Singh [35] studied about MF lubricated porous pivoted slider bearing with slip velocity. There it was discussed about the minimization of the slip parameter and permeability parameter for the possible increase in the load capacity. Andharia and Deheri [36] studied MF based squeeze-film for truncated conical plates with the effect of longitudinal roughness and found that load capacity can be increased with magnetization as well as negatively skewed roughness. The pressure and response time also found to increase with magnetization. Singh and Gupta [37] studied about curved slider bearing with FF as

lubricant and shown that the effect of rotation and volume concentration of magnetic particles improves the stiffness and damping capacities of the bearings. Lin *et. al.* [38] studied squeeze-film characteristics for conical plates with the effect of fluid inertia and FF, and shown the better performance of the system as compared to non-inertia non-magnetic case. Lin *et. al.* [39] studied squeeze-film characteristics of parallel circular discs with the effects of FF and non-Newtonian couple stresses using transverse magnetic field. With these effects, it was shown that higher load capacity and lengthens approaching time obtained. Andharia and Deheri [40] studied about performance of a MF based squeeze-film between longitudinally rough elliptical plates. It was observed that increase in load-carrying capacity due to MF lubricant gets considerably increased due to the combined effect of standard deviation and negatively skewed roughness. Lin *et. al.* [41] studied effects of circumferential and radial roughness in the study of squeeze-film using non-Newtonian MF. It was shown that the mean load-carrying capacity increases and prolongs the mean approaching time as compared to those of the smooth discs with a non-Newtonian MF. However, in the case of radial roughness pattern the above trend is reverse. Huang and Wang [42] presented a comprehensive review on FFs lubrication theory based on different flow models. Shah and co-authors [43-53] studied about FF lubricated various designed bearings like porous slider bearings of different shapes, long journal bearing, axially undefined journal bearing, squeeze-film-bearings with the inclusion of effects of slip velocity at the porous boundary and anisotropic permeability of the porous matrix attached to the impermeable plate.

Because of having significant effect of surface roughness on the bearing performances, the present Chapter studied FF lubricated squeeze-film behaviour formed

between a rotating upper sphere and a radially rough lower flat plate (disc or surface) considering variable magnetic field which is oblique to the lower plate. The variable magnetic field is important because of its advantage of generating maximum field at the required active contact zone. The FF considered here is water based. On the basis of ferrohydrodynamic theory and Christensen's stochastic theory for hydrodynamic lubrication of rough surfaces, the modified Reynolds equation is derived and expressions for squeeze-film characteristics are obtained and calculated numerically. The effects of various parameters like radial co-ordinates, radial roughness, rotation, width of the nominal minimum film thickness and squeeze velocity are also considered and studied.

4.2 Mathematical Formulation and Solution

The schematic diagram of the squeeze-film geometry under study is shown in figure 4.1. A rigid rotating sphere of radius a is approaching towards radially rough flat plate with a uniform velocity (known as squeeze velocity)

$$\dot{h}_0 = \frac{dh_0}{dt},$$

(4.1)

under a constant load, where h_0 is the central film thickness at time $t=0$. As shown in figure 4.1   the gap between a sphere and a plate (known as film region or film thickness) is filled with FF lubricant which is controlled by oblique (oblique to the lower plate) and variable magnetic field of strength H of the form [43]

$$H^2 = \frac{Kr^2(a-r)}{a},$$

(4.2)

where r is the radial co-ordinate and K being a quantity chosen to suit the dimensions of both sides of equation (4.2) which helps in getting maximum magnetic field strength at $r = 2\,a\,/\,3$ as follows .

From equation (4.2),

$$Max.\ H^2 = 0.21 \times 10^{-4} K \quad for \quad a{=}0.012,$$

which implies for

$$K = \frac{10^{10}}{0.21}, \text{ so that } H \approx O(10^3) \text{ or } O(H) \approx 3,$$

where O indicates order.

Also,

$$\mathbf{q} = (\dot{r}, r\dot{\theta}, \dot{z}) = (u, rv, w),$$

(4.3)

where (r, θ, z) are cylindrical polar co-ordinates and dot (.) represents derivative w.r.t. t.

For an incompressible, steady, axisymmetric flow, equations (2.25) to (2.29) with equation (4.3) in cylindrical polar co-ordinates in r-direction becomes

$$-\frac{v^2}{r} = -\frac{1}{\rho}\frac{\partial}{\partial r}\left(p - \frac{1}{2}\mu_0\bar{\mu}H^2\right) + \frac{\eta}{\rho}\frac{\partial^2 u}{\partial z^2},$$

(4.4)

under the usual assumptions of lubrication, neglecting inertia terms and that the derivatives of fluid velocities across the film predominate.

Using tangential velocity under the boundary conditions

$$v = r\Omega_l \quad when \quad z = 0$$

and

$$v = r\,\Omega_u \quad \text{when } z = h,$$

equation (4.4) becomes

$$-r\left(\frac{z}{h}\Omega_r + \Omega_l\right)^2 = -\frac{1}{\rho}\frac{\partial}{\partial r}\left(p - \frac{1}{2}\mu_0\bar{\mu}H^2\right) + \frac{\eta}{\rho}\frac{\partial^2 u}{\partial z^2}; \ \Omega_r = \Omega_u - \Omega_l,$$

(4.5)

which on simplification yields

$$\frac{\partial^2 u}{\partial z^2} = \frac{1}{\eta}\left[\frac{\partial}{\partial r}\left(p - \frac{1}{2}\mu_0\bar{\mu}H^2\right) - \rho r\left(\frac{z}{h}\Omega_r + \Omega_l\right)^2\right],$$

(4.6)

where Ω_l is the rotation of the lower plate, Ω_u is the rotation of the upper sphere and h is the film thickness made up of two parts

$$h = h_n(r) + h_s(r,\theta,\xi) \ ;$$

(4.7)

h_n denotes the nominal smooth part of the film geometry and is defined as [10,22]

$$h_n = h_m + \frac{r^2}{2a},$$

(4.8)

provided $r << a$, h_m being the nominal minimum film thickness at r=0 and $h_s(r,\theta,\xi)$ is the part due to the surface asperities measured from nominal level and is a randomly varying quantity with zero mean, ξ being an index determining a definite roughness arrangement .

Solving equation (4.6) for u with the corresponding boundary conditions

$$u = 0 , \quad w = 0 \quad \text{when} \quad z = 0$$

and

$$u = 0 , w = -\frac{dh_0}{dt} \quad \text{when } z = h,$$

$$(4.9)$$

yields

$$u = \frac{1}{\eta}\left[\frac{\partial}{\partial r}\left(p - \frac{1}{2}\mu_0\bar{\mu}H^2\right)\left(\frac{z^2}{2} - \frac{hz}{2}\right) - \rho\, r\Omega_r^2\left(\frac{z^4}{12h^2} - \frac{hz}{12}\right) - \left(\frac{z^3}{3h} - \frac{hz}{3}\right)\rho\, r\Omega_r\Omega_l - \left(\frac{z^2}{2} - \frac{hz}{2}\right)\rho\, r\Omega_l^2\right].$$

$$(4.10)$$

The continuity equation (2.26) for the film region in cylindrical polar co-ordinates yields

$$\frac{1}{r}\frac{\partial}{\partial r}(ru) + \frac{\partial w}{\partial z} = 0.$$

$$(4.11)$$

Substituting equation (4.10) in equation (4.11) and integrating over the film thickness $(0, h)$ using boundary conditions for w from (4.9), yields Reynolds type equation of the form

$$\frac{1}{r}\frac{\partial}{\partial r}\left[rh^3\frac{\partial}{\partial r}\left(p - \frac{1}{2}\mu_0\bar{\mu}H^2\right)\right] = \frac{1}{r}\frac{\partial}{\partial r}\left[h^3\rho\, r^2\left(\frac{3}{10}\Omega_r^2 + \Omega_r\Omega_l + \Omega_l^2\right)\right] - 12\eta\frac{dh_0}{dt},$$

$$(4.12)$$

where the fact that

$$w_0 = w\big|_{z=0} = 0,$$

Because rough plate is solid.

Let $f(h_s)$ be the probability density function of the stochastic film thickness, h_s .Taking the stochastic average of equation (4.12) with respect to $f(h_s)$, the stochastic Reynolds equation can be obtained in the form

$$\frac{1}{r}\frac{\partial}{\partial r}\left[rE(h^3)\frac{\partial}{\partial r}\left\{E(p)-\frac{1}{2}\mu_0\bar{\mu}H^2\right\}\right]=\frac{1}{r}\frac{\partial}{\partial r}\left[E(h^3)\rho r^2\left(\frac{3}{10}\Omega_r^2+\Omega_r\Omega_l+\Omega_l^2\right)\right]-12\eta\frac{dh_0}{dt},$$

(4.13)

where $E(*)$ is the expectancy operator defined by

$$E(*)=\int_{-\infty}^{\infty}(*)f(h_s)dh_s .$$

(4.14)

After Christensen [15], it is assumed that

$$f(h_s)=\begin{cases}\dfrac{35}{32c^7}(c^2-h_s^2)^3, & -c<h_s<c\\[2mm]0 & , \quad \text{elsewhere}\end{cases}$$

(4.15)

where $\sigma=c/3$ is the standard deviation.

In the context of stochastic theory, the analysis is usually done for two types of one-dimensional roughness pattern (viz. circumferential and radial). In this Chapter, one dimensional radial roughness pattern is considered for study. For this pattern, the roughness structure is having the form of long, narrow ridges and valleys running in r-direction (that is, they are straight ridges and valleys passing through $z = 0$, $r = 0$ to form a star pattern). The film thickness in this case assumes the form

$$h = h_n + h_s(\theta, \xi),$$

(4.16)

so that the stochastic Reynolds equation becomes

$$\frac{1}{r}\frac{\partial}{\partial r}\left[rE(h^3)\frac{\partial}{\partial r}\left\{E(p) - \frac{1}{2}\mu_0\overline{\mu}\,H^2\right\}\right] = \frac{1}{r}\frac{\partial}{\partial r}\left[E(h^3)\,\rho r^2\left(\frac{3}{10}\Omega_r^2 + \Omega_r\Omega_l + \Omega_l^2\right)\right] - 12\eta\frac{dh_0}{dt},$$

(4.17)

where

$$E(h^3) = h_n^3 + \frac{1}{3}h_n c^2.$$

(4.18)

Introducing the dimensionless quantities

$$R = \frac{r}{a}, \quad V = \frac{\dot{h}_0}{\Omega_u h_0}, \quad S = -\frac{\rho\Omega_u h_0^2}{\eta V}, \quad \overline{h}_n = \frac{h_n}{h_0}, \quad \overline{p} = -\frac{E(p)h_0^3}{a^2\eta\dot{h}_0}, \quad \overline{a} = \frac{a}{h_0}$$

$$\overline{h}_s = \frac{h_s}{h_0}, \quad \overline{h}_m = \frac{h_m}{h_0}, \quad \overline{h} = \frac{h}{h_0}, \quad \Omega_f = \frac{\Omega_l}{\Omega_u}, \quad C = \frac{c}{h_0}, \quad \mu^* = -\frac{K\mu_0\overline{\mu}\,h_0^3}{\eta\dot{h}_0}$$

(4.19)

The stochastic Reynolds equation (4.17) reduces to

$$\frac{1}{R}\frac{\partial}{\partial R}\left[RF\frac{\partial}{\partial R}\left\{\overline{p} - \frac{1}{2}\mu^*R^2(1-R)\right\}\right] = \frac{1}{R}\frac{\partial}{\partial R}(GR),$$

(4.20)

$$F = \overline{h}_n^3 + \frac{1}{3}\overline{h}_n C^2,$$

(4.21)

$$G = R\,S\left(\bar{h}_n^3 + \frac{1}{3}\bar{h}_n C^2\right)\left(\frac{3 + 4\Omega_f + 3\Omega_f^2}{10}\right) + 6R.$$

Also, equations (4.2), (4.8) and (4.16) can be written as

$$H^2 = K a^2 R^2 (1 - R) \quad,\quad \bar{h}_n = \bar{h}_m + \frac{R^2 \bar{a}}{2} \quad \text{and} \quad \bar{h} = \bar{h}_n + \bar{h}_s,$$

respectively.

4.2.1 Pressure Distribution

Solving equation (4.20) for the following relevant boundary conditions

$$\bar{p} = 0 \quad \text{when } R = 1,$$

and

$$\frac{\partial \bar{p}}{\partial R} = 0 \quad \text{when } R = 0,$$

yields dimensionless film pressure as

$$\bar{p} = \frac{1}{2}\mu^* R^2 (1 - R) - \int_R^1 \frac{G}{F}\,dR.$$

4.2.2 Load-Carrying capacity

The mean load-carrying capacity is derived by integrating the mean film pressure acting on the sphere and is given by

$$E(W) = 2\pi \int_0^a E(p) r dr$$

$$= -\frac{2\pi a^4 \eta \dot{h}_0}{h_0^3} \int_0^1 \overline{p} \, R \, dR.$$

(4.25)

Thus, the dimensionless load-carrying capacity can be obtained as

$$\overline{W} = -\frac{h_0^3 E(W)}{2\pi \eta a^4 \dot{h}_0} = \int_0^1 \overline{p} \, R \, dR = \frac{\mu^*}{40} - \frac{1}{2} \int_0^1 \frac{G}{F} R^2 dR,$$

(4.26)

where F and G are given by equations (4.21) and (4.22) respectively.

4.3 Results and Discussion

In the present analysis, squeeze-film between a rotating upper sphere and a radially rough lower flat plate is analyzed using FF as lubricant. The dimensionless film pressure ($\overline{p}$) is studied for the effect of dimensionless radial co-ordinate R. Moreover, the Chapter also studied about the effects of dimensionless radial surface roughness parameter, rotational parameter, width of the nominal minimum film thickness and squeeze velocity on dimensionless load-carrying capacity ($\overline{W}$). The radial roughness model considered here is based on Christensen's stochastic theory [15] for hydrodynamic lubrication of rough surfaces. The FF considered here is water based. The magnetic field is oblique and variable to the lower plate. This type of magnetic field is important because of its advantage of generating maximum field at the required active contact zone. The strength of the magnetic field considered throughout the study is of order 3; that is, $O(H) \approx 3$ in order to get maximum field strength at $r = 2a/3$. When FF is used as

lubricant, the variation in $\bar{p}$ and $\overline{W}$ is due to the first term of the equations (4.24) and (4.26) respectively. The values of the dimensionless film pressure and load-carrying capacity have been calculated for the following value of different parameters [10,54,55] which are remain fixed whenever required during calculation.

$$K = 10^{10}/0.21\,(\text{A}^2\ \text{m}^{-4}),\ h_m = 0.00025\,(\text{m}),\ \rho = 1400\ (\text{Ns}^2\text{m}^{-4})$$

$$\bar{\mu} = 0.05,\ \eta = 0.012\ (\text{Ns m}^{-2}),\ a = 0.012\,(\text{m}),\ \mu_0 = 4\pi \times 10^{-7}\,(\text{NA}^{-2})$$

$$h_0 = 0.00035\ (\text{m}),\ \dot{h}_0 = 0.001\,(\text{ms}^{-1}),\ \Omega_u = 30\pi\ (\text{rad.s}^{-1}),\ \Omega_l = 30\pi\ (\text{rad. s}^{-1}),$$

$$\pi = 22/7,\ r = 0.0006\ (\text{m})$$

Chan and Horn [9] in 1985 considered Reynolds lubrication equation when sphere of radius R moving normally towards a flat surface at a separation h_0 and shown that the pressure distribution $p(r)$ over the spherical surface satisfies the equation

$$\frac{1}{r}\frac{d}{dr}\left[r\,h_n^3\,(r)\frac{dp(r)}{dr}\right] = 12\eta\,\dot{h}_m,$$

$$(4.27)$$

where $h_n(r)$ is the separation of the surface at a radius r and is given by equation (4.8).

Matthewson [10] in 1988 discussed about the analytical derivation for the squeeze flow of the liquid bridge of Newtonian fluid between a smooth rigid sphere and a smooth rigid flat plate using equation (4.27). Naduvinamani $et.\ al.$ [22] in 2005 studied about the effect of roughness on the squeeze-film between a sphere and a flat plate using couple-stress fluid. Here, they have derived the Reynolds equation giving pressure distribution of the form

$$\frac{1}{r}\frac{\partial}{\partial r}\left[r\left\{h^3+\frac{12h}{\tau^2}+\frac{24}{\tau^3}\tanh\left(\frac{\tau h}{2}\right)\right\}\frac{dp}{dr}\right]=12\eta\dot{h},$$

(4.28)

where τ is the inverse of the microstructural length scale responsible for the couple-stress effect and h is given by equation (4.7). Equation (4.28) can be reduced to equation (4.27) when there is no roughness effect and Newtonian fluid is used.

Considering base as equations (4.27) and (4.8), the present study is the extension of the work by Chan and Horn [9] as well as Naduvinamani *et. al.* [22] in the context of Reynolds equation for pressure distribution and addition of roughness pattern respectively. The Chapter also considers FF as lubricant with oblique and variable magnetic field instead of conventional as well as couple-stress fluid and also rotation effect of the sphere.

The results for dimensionless film pressure ($\bar{p}$) is calculated with respect to dimensionless radial co-ordinate R whereas the results for dimensionless load-carrying capacity ($\overline{W}$) is calculated with respect to different dimensionless parameters like radial surface roughness, rotation of the sphere and a flat plate, width of the nominal minimum film thickness and squeeze velocity. The results are presented graphically.

4.3.1 Discussion on Dimensionless Film Pressure

Figure 4.2 shows the variation of $\bar{p}$ as a function of dimensionless radial parameter (R) when radial surface roughness parameter C=0.004286, rotational parameter $\Omega_f = 1$ and $O(H)\approx 3$. It is observed that $\bar{p}$ decreases as R increases; that is, as radius of the sphere a decreases since $R = r/a$. This decrease nature of $\bar{p}$ agrees with the behaviour of [22]. It should be noted here that as per [22], when $R = 0.1$, $C \approx 0.2$ then $\bar{p} \approx 5.5$

while in our case $\bar{p} \approx 21.7$ when $R = 0.1$, C=0.004286. Hence, approximate benefit of 294.5 % more pressure generation is obtained even if smaller value of surface roughness parameter C is assigned, which is the advantage of the present method. From figure maximum pressure can be generated when R is nearer to 0.02 which can be obtained when $r = 0.0006$ m and $a = 0.03$ m; that is, $r << a$, which is the basic requirement of this problem [10]. Thus, the value of a is considered about 4900 % more than the value of r. The integral in equation (4.24) can be solved using Simpson's 1/3-rule with step size determined by the formula $(1-R)/10$.

4.3.2 Discussion on Dimensionless Load-Carrying Capacity

Before proceeding further, it should be noted that the integral in equation (4.26) can be solved using Simpson's 1/3-rule with step size 0.1.

Figure 4.3 shows the variation of dimensionless load-carrying capacity ($\overline{W}$) as a function of dimensionless radial surface roughness parameter (C) for different values of rotational parameter (Ω_f). It is observed that with the present variation in radial surface roughness pattern, there is negligible effect on $\overline{W}$ which also remains same for $C = 0$. However, in the case of Naduvinamani [22], the radial roughness pattern cause decrease in $\overline{W}$ as compared to smooth case (C=0). Thus, the added advantage of constant behaviour of $\overline{W}$ whether $C = 0$ or $C \neq 0$ is obtained as compared to [22].

Figure 4.4 shows the variation of $\overline{W}$ as a function of dimensionless rotational parameter (Ω_f) for C=0.004286 when $\Omega_l > \Omega_u$; that is, when lower plate is rotated faster than upper sphere since $\Omega_f = \Omega_l / \Omega_u$. It is observed that $\overline{W}$ increases as Ω_f increases along the positive axis as well as decreases along the negative axis. That is, $\overline{W}$

increases when the rotation of the lower plate increases counterclockwise or clockwise. But the increase rate is more in the case of counterclockwise rotation. Table 4.1 show the maximum value of $\overline{W}$ for the calculated domain, when lower plate is rotated in different directions.

Thus, it is observed that the increase rate of $\overline{W}$ is possible more than 186.03% in the case of counterclockwise rotation of the lower plate.

Figure 4.5 shows the variation of $\overline{W}$ as a function of dimensionless rotational parameter(Ω_f) for C=0.004286 when $\Omega_l \leq \Omega_u$ (excluding the case $\Omega_f = 0$; that is, $\Omega_l = 0$); that is, when upper sphere is rotated faster than lower plate. It is observed that $\overline{W}$ decreases as Ω_f increases along the positive axis as well as decreases along negative axis. That is, $\overline{W}$ increases as the rotation of the upper sphere increases counterclockwise as well as clockwise. But as in the case of figure 4.4, the increase rate of $\overline{W}$ is more in the case of counterclockwise rotation. Table 4.2 show the maximum value of $\overline{W}$ for the calculated domain, when upper sphere is rotated in different directions.

Thus, the percentage increase in $\overline{W}$ is again 186.03% when the upper sphere is rotated in counterclockwise direction. This is because the kinematics of rotation remains same in both the cases.

When $\Omega_f = 0$; that is, when there is no rotation of the lower plate irrespective of the rotation of the upper sphere, $\overline{W}$ is observed to be increases when the rotation of the above sphere increases either counterclockwise or clockwise directions as can be seen from Table 4.3.

Figure 4.6 shows the variation of $\overline{W}$ as a function of dimensionless nominal minimum film thickness ($\bar{h}_m$) when C=0.004286 and $\Omega_f = 1$. It is observed that $\overline{W}$ increases as $\bar{h}_m$ increases; that is, $\overline{W}$ increases as nominal minimum film thickness increases. But the increase rate of $\overline{W}$ is marginal. Figure 4.7 shows the variation of $\overline{W}$ as a function of dimensionless squeeze velocity parameter (V) when C=0.004288 and $\Omega_f = 1$. It is observed that $\overline{W}$ decreases as V increases. Also, it is observed that smaller squeeze velocity results into more $\overline{W}$ and the best performance of $\overline{W}$ is obtained when $0 < V < 0.025$. For $V > 0.025$, $\overline{W}$ decreases slowly.

The present case reduces to the case of Naduvinamani *et.al.* [22] when there is no rotation effect at both (upper and lower) surfaces and FF lubricant is replaced by couple-stress fluid. The case will further deduce to Lin [56], when there is no surface roughness effect in addition.

4.4 Conclusions

On the basis of ferrohydrodynamic theory and Christensen's stochastic theory for hydrodynamic lubrication of rough surfaces, a water based FF lubricated squeeze-film bearing design system formed between a rotating upper sphere and a radially rough lower flat plate is analysed for the study of effects of roughness, rotation, width of the nominal minimum film thickness and squeeze velocity on dimensionless load-carrying capacity ($\overline{W}$). The dimensionless film pressure distribution ($\bar{p}$) is also discussed with respect to radial coordinate. The variable magnetic field oblique to the lower plate is considered here for study because during cause of investigation it is observed that uniform magnetic

field does not enhance bearing performances (refer equation (4.5)). Moreover, the variable magnetic field is important because of its advantage of generating maximum magnetic field at the required active contact zone of the bearing design system. The analytic model, known as Reynolds equation, is derived using equation of continuity and equations from ferrohydrodynamic theory. The following conclusions can be made from results and discussion.

1. The influence of water based FF as lubricant which is controlled by oblique and variable magnetic field gives positive effect on the overall performance of the present sphere-plate system.

2. $\bar{p}$ increases as R decreases; that is, as radius of the sphere a increases.

3. $\overline{W}$ remains almost constant with the variation of roughness parameter.

4. $\overline{W}$ increases when the rotation of the upper sphere or lower plate increases counterclockwise or clockwise. But the maximum value of $\overline{W}$ is obtained when the rotation is counterclockwise. Moreover, $\overline{W}$ increases even if rotation of the lower plate is zero irrespective of the increase of rotation of the upper sphere.

5. $\overline{W}$ increases with the increase of nominal minimum film thickness but the increase rate is marginal.

6. $\overline{W}$ increases when squeeze velocity decreases and the better performance is obtained when $0 < V < 0.025$.

4.5 Tables

	Ω_f	$\overline{W}$
Counterclockwise	2.33	15.93
Clockwise	-2.33	5.55
% increase in $\overline{W}$		187.03

Table 4.1

Values of $\overline{W}$ when lower plate is rotated in different directions

-

	Ω_f	$\overline{W}$
Counterclockwise	0.43	15.93
Clockwise	-0.43	5.55
% increase in $\overline{W}$		187.03

Table 4.2

Values of $\overline{W}$ when upper sphere is rotated in different directions

Ω_f	30π	40π	50π	60π	70π
	-30π	-40π	-50π	-60π	-70π
$\overline{W}$	1.66	2.96	4.63	6.67	9.08

Table 4.3

Effects on $\overline{W}$ when the rotation of the lower plate is zero irrespective of the rotation of

the upper sphere

4.6 Figures

Figure 4.1

Ferrofluid based squeeze-film geometry between a sphere and a

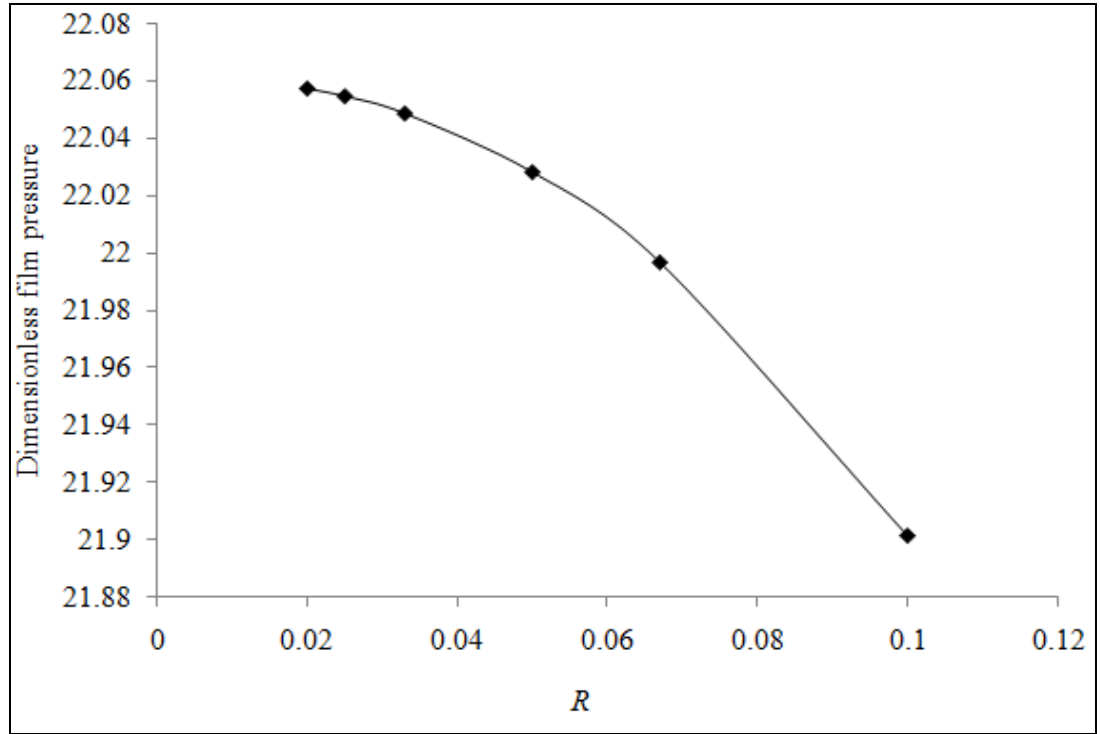radially rough flat plate with oblique and variable magnetic field

Figure 4.2

Variation in dimensionless film pressure $\bar{p}$ for different values of dimensionless radial

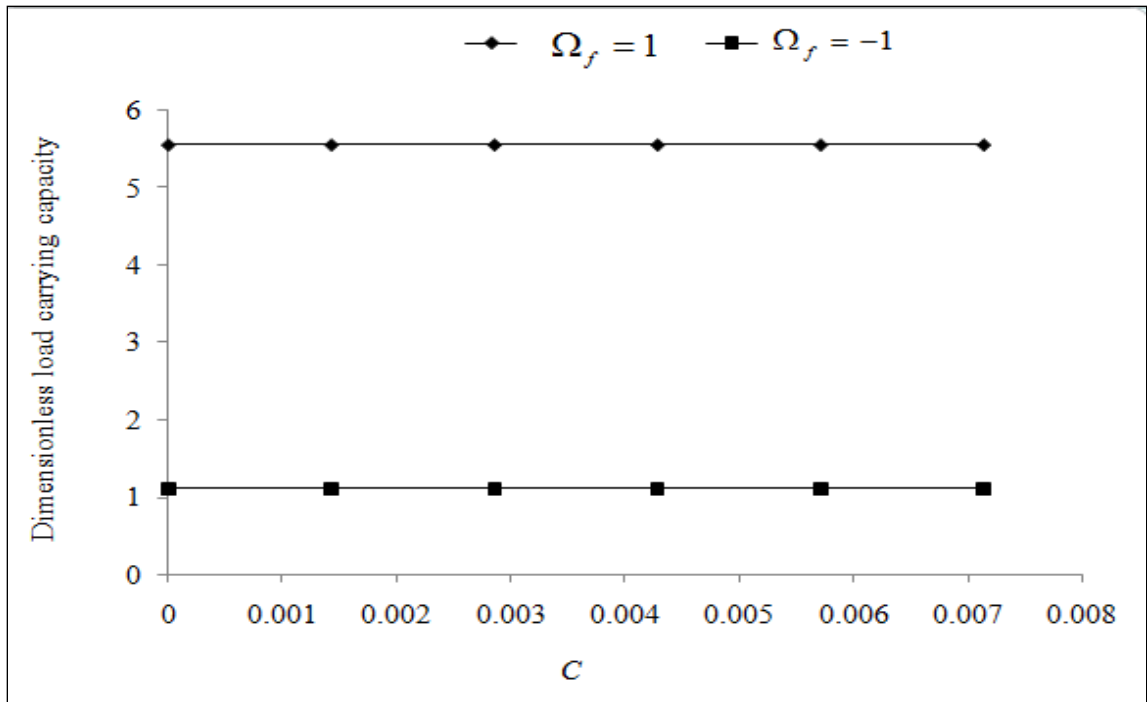co-ordinate R considering C=0.004286, Ω_f = 1 and $O(H) \approx 3$

Figure 4.3

Variation in dimensionless load-carrying capacity $\overline{W}$ for different values of radial surface
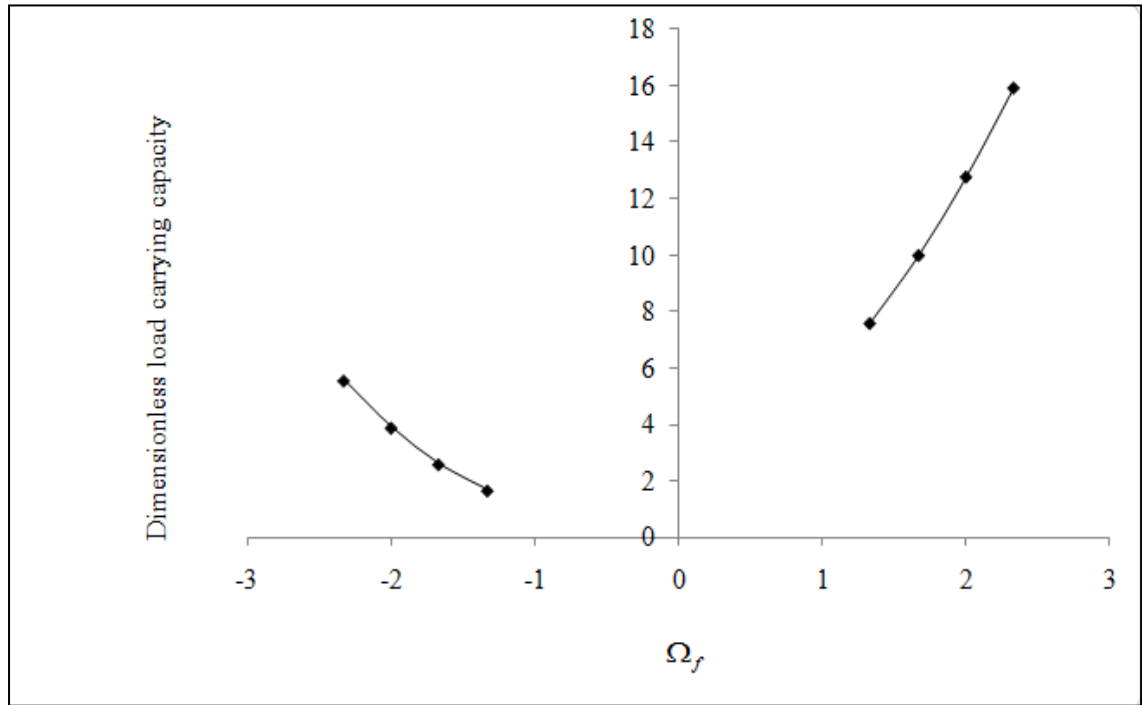
roughness parameter C and rotational parameter Ω_f

Figure 4.4

Variation in dimensionless load-carrying capacity $\overline{W}$ for different values of rotational

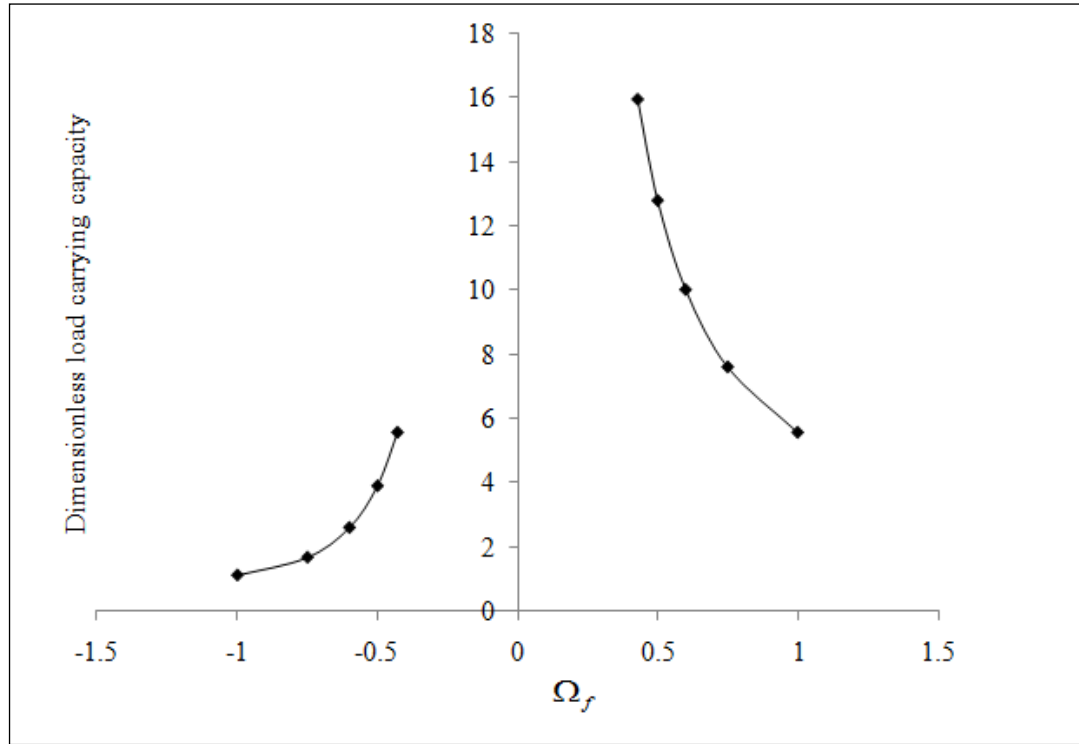parameter Ω_f considering $\Omega_l > \Omega_u$ and $C{=}0.004286$

Figure 4.5

Variation in dimensionless load-carrying capacity $\overline{W}$ for different values of rotational parameter Ω_f considering $\Omega_l \leq \Omega_u$ and C=0.004286
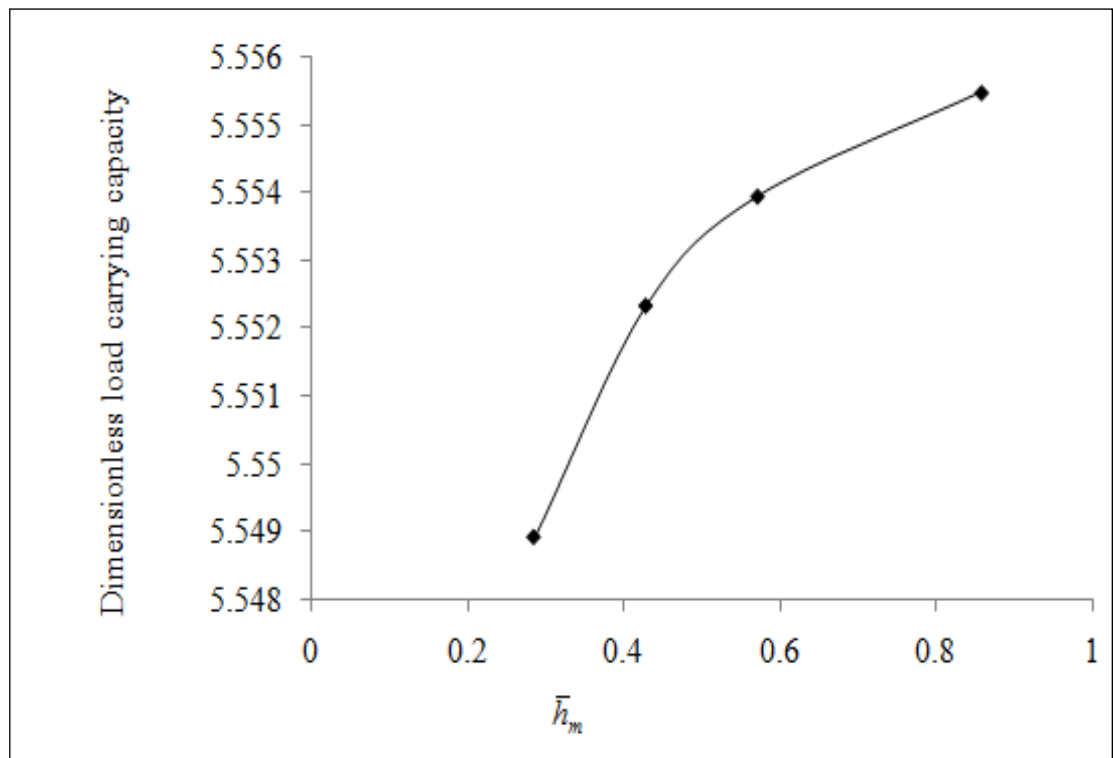
Figure 4.6

Variation in dimensionless load-carrying capacity $\overline{\overline{W}}$ for different values of

dimensionless nominal minimum film thickness $\overline{h}_m$ considering C=0.004286 and
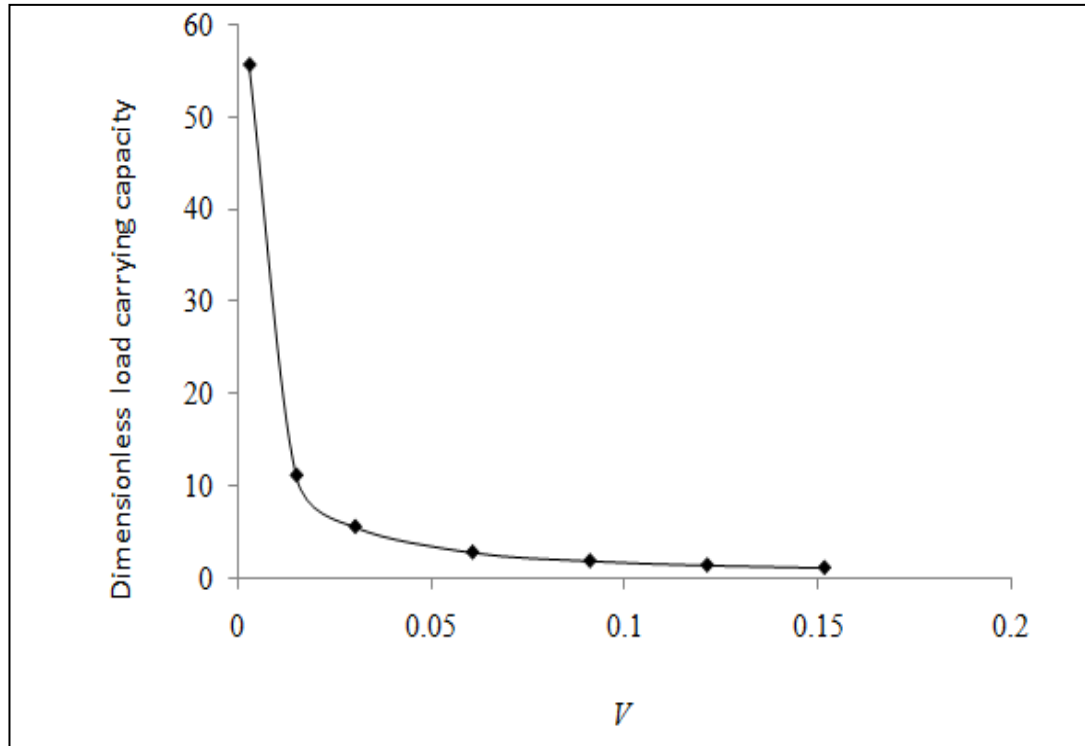
$$\Omega_f = 1$$

Figure 4.7

Variation in dimensionless load-carrying capacity $\overline{W}$ for different values of

dimensionless squeeze velocity parameter V considering C=0.004288 and $\Omega_f = 1$

4.7 References

[1]   P. Gould, Parallel surface squeeze-films: The effect of the variation of the viscosity with temperature and pressure, *Journal of Lubrication Technology* (1967) 375-380.

[2]   O. Reynolds, On the theory of lubrication and its application to Mr.   Beauchamp tower's experiments, including an experimental determination of the viscosity of olive oil, *Philosophical Transactions of the Royal Society of London, Series A* 177 (1886) 157-234.

[3]   F.R. Archibald, Load capacity and time relations for squeeze-films, *Transactions of ASME* 78 (1956) 29-35.

[4]   J.D. Jackson, A Study of squeezing flow, *Applied Scientific Research,   Section A* 11 (1963) 148-152.

[5]   D.F. Moore, Review of squeeze-films, *Wear* 8 (1965) 245-263.

[6]   H. Christensen, Elastohydrodynamic theory of spherical bodies in normal   approach, *Journal of lubrication Technology* 92 (1970) 145-154.

[7]   P. Gould, High-pressure spherical squeeze-films, *Journal of Lubrication Technology* 92 (1971) 207-208.

[8]   D. Conway and H.C. Lee, Impact of a lubrication surface by a sphere, *Journal of Lubrication Technology* 97 (1975) 613-615.

[9]   D.Y.C. Chan and R.G. Horn, The drainage of thin liquid films between solid Surfaces, *Journal of Chemical Physics* 83 (1985) 5311-24.

[10]   M.J. Matthewson, Adhesion of spheres by thin liquid films, *Philosophical Magazine A* 57(2) (1988) 207-16.

[11]   G.H. Meeten, Squeeze flow between plane and spherical surfaces, *Rheologica Acta* 40 (2001) 279-288.

[12]   R. A. Burton, Effect of two–dimensional, sinusoidal roughness on the   load support characteristics of a lubricant film, *Journal of Basic   Engineering* 85(2) (1963) 258.

[13]   Davies, The generation of pressure between rough fluid lubricated,   moving, deformable surfaces, *Lubrication of Engineering* 19 (1963) 246.

[14]   S.T. Tzeng and E. Saibel, Surface roughness effect on slider bearing lubrication,   *ASLE Transaction 10 (1967) 334.*

[15]   H. Christensen, Stochastic model for hydrodynamic lubrication of rough surfaces*, Proceedings of the Institute of Mechanical Engineers (part J)* 184(55) (1970) 1013-1026.

[16]   K. Tonder, Surface distributed waviness and roughness, *Proceedings of the first world conference in industrial Tribology*, New Delhi (1972) 1-8.

[17]   H. Christensen and K. Tonder, The hydrodynamic lubrication of rough journal bearings, *Trans. ASME Journal of Lubrication Technology* 95 (1973) 166-172.

[18]   J. Prakash and H. Christensen, Squeeze-films between two rough rectangular plates, *Journal of Mechanical Engineering Science* 20(4) (1978) 183-188.

[19]   J. Prakash and K. Tiwari, Lubrication of a porous bearing with surface corrugations, *Journal of lubrication Technology* 104 (1982) 127-134.

[20]   P.I. Andharia, J.L. Gupta and G.M. Deheri,   Effect of tansverse surface roughness on the   behaviour of squeeze film in a spherical bearing, *Applied Mechanics and Engineering* 4 (1999) 19-24.

[21]   J.R. Lin, C.H. Hsu and C. Lai, Surface roughness effects on the oscillating squeeze-film behaviour of long partial journal bearings, *Computers and Structures* 80 (2002) 297-303.

[22]   N.B. Naduvinamani, P.S. Hiremath and G. Gurubasavaraj, Effect of surface roughness on the Couple-stress squeeze-film between a sphere and a flat plate, *Tribology International* 38 (2005) 451-458.

[23]   N.M. Bujurke, D.P. Basti and R.B. Kudenatti, Surface roughness effects on squeeze-film behaviour in porous circular disks with couple stress fluid, *Transport in Porous Media* 71 (2008) 185-197.

[24]   D.P. Basti, Effect of surface roughness and couple stresses on squeeze-films between curved annular plates, *ISRN Tribology* (2013) Article ID 640178: 8 pages.

[25]   R.E. Rosensweig, Ferrohydrodynamics, New York: *Cambridge University Press*, 1985.

[26]   V.G. Bashtovoi and B.M. Berkovskii, Thermomechanics of ferromagnetic fluids, *Magnitnaya Gidrodinamika* 3 (1973) 3-14.

[27]   M. Goldowsky, New methods for sealing, filtering, and lubricating with magnetic fluids, *IEEE Transactions on Magnetics*, *Mag*. 16 (1980) 382-386.

[28]   N.C. Popa, I. Potencz, L.Brostean and L.Vekas, Some applications of inductive Transducers with magnetic fluids, *Sensors and Actuators A*   59 (1997) 197-200.

[29]   R.V. Mehta and R.V. Upadhyay, Science and technology of ferrofluids, *Current Science* 76(3) (1999) 305-312.

[30]   J. Liu, Analysis of a porous elastic sheet damper with a magnetic fluid,

Journal   of Tribology 131 (2009) 0218011-15.

[31]   V.K. Agrawal, Magnetic fluid based porous inclined slider bearing, *Wear* 107 (1986) 133-139.

[32]   C.Q. Chi, Z.S. Wang and P.Z. Zhao, Research on a new type of ferrofluid – lubricated journal bearing, *Journal of Magnetism and Magnetic Materials* 85 (1990) 257-260.

[33]   P. Sinha, P. Chandra and D. Kumar, Ferrofluid lubrication of cylindrical rollers with cavitation, *Acta Mechanica* 98 (1993) 27-38.

[34]   E. Uhlmann ,G. Spur, N. Bayat and R. Patzwald , Application of magnetic fluids in tribotechnical systems, *Journal of Magnetism and Magnetic Materials* 252 (2002) 336–340.

[35]   N. Ahmad and J.P. Singh, Magnetic fluid lubrication of porous-pivoted slider bearing with slip velocity, *Journal of Engineering Tribology* 221 (2007) 609-613.

[36]   P.I. Andharia and G.M. Deheri, Effect of longitudinal roughness on magnetic fluid based squeeze-film between truncated conical plates, *FDMP* 7(1) (2011) 111-124.

[37]   U.P. Singh and R.S. Gupta, Dynamic performance characteristics of a curved slider bearing operating with ferrofluids, *Advances in Tribology* (2012) Article ID 278723: 6 pages.

[38]   J.R. Lin, M.C. Lin , T.C. Hung and P.Y.Wang, Effects of fluid inertia forces on the squeeze-film characteristics of conical plates-ferromagnetic fluid model, *Lubrication Science* 25 (2013) 429-439.

[39]   J.R. Lin, R.F. Lu, M.C. Lin and P.Y. Wang, Squeeze-film characteristics of parallel circular disks lubricated by ferrofluids with non-Newtonian couple stresses, *Tribology International* 61 (2013) 56-61.

[40]   P.I. Andharia and G.M. Deheri, Performance of magnetic-fluid-based squeeze-film between longitudinally rough elliptical plates, *ISRN Tribology* 2013; Article ID 482604, 6 pages.

[41]   J.R. Lin, L.J. Liang ,M.C. Lin and S.T.Hu, Effects of circumferential and radial rough surfaces in a non-Newtonian magnetic fluid lubricated squeeze film, *Applied Mathematical Modelling* 39 (2015) 6743-6750.

[42]   W. Huang and X. Wang, Ferrofluids lubrication : a status report, *Lubrication Science* 28 (2016) 3-26.

[43]   R.C. Shah and M.V. Bhat, Squeeze-film based on magnetic fluid in curved porous rotating circular plates, *Journal of Magnetism and Magnetic Materials* 208 (2000) 115–119.

[44]   R.C. Shah and M.V. Bhat, Ferrofluid lubrication in porous inclined, slider bearing with velocity slip, *International Journal of Mechanical Sciences* 44 (2002) 2495-2502.

[45]   R.C. Shah and M.V. Bhat, Porous secant shaped slider bearing with slip velocity lubricated by ferrofluid, *Industrial Lubrication Tribology* 55(3) (2003) 113-115.

[46]   R.C. Shah and M.V. Bhat, Ferrofluid squeeze-film in a long journal bearing, *Tribology International* 37 (2004) 441- 446.

[47]   R.C. Shah and M.V. Bhat, Ferrofluid lubrication of a porous slider bearing with a convex pad surface considering slip velocity, *International Journal of Applied*

Electromagnetics and Mechanics 20 (2004) 1-9.

[48]   R.C. Shah and M.V. Bhat, Anisotropic permeable porous facing and slip velocity on squeeze-film in an axially undefined journal bearing with ferrofluid lubricant, *Journal of Magnetism and Magnetic Materials* 279 (2004) 224-230.

[49]   R.C. Shah and M.V. Bhat, Magnetic fluid lubrication of bearing, each having a porous faced stator and a slider having various shapes, *Magnetohydrodynamics* 40(1) (2004) 91-97.

[50]   R.C. Shah and D.B. Patel, Mathematical analysis of newly designed ferrofluid lubricated double porous layered axially undefined journal bearing with anisotropic permeability, slip velocity and squeeze velocity, *International Journal of Fluid Mechanics Research* 40(5) (2013) 446-454.

[51]   R.C. Shah and D.B. Patel, Magnetic fluid lubrication of porous pivoted slider bearing with slip and squeeze velocity, *International Journal Industrial Mathematics* 6(3) (2014) 199-206.

[52]   R.C. Shah and R.C. Kataria, Mathematical analysis of newly designed two porous layers slider bearing with a convex pad upper surface considering slip and squeeze velocity using ferrofluid lubricant, *International Journal of Mathematical Modelling & Computations* 04(02) (2014) 93-101.

[53]   R.C. Shah and N.I. Patel, Impact of various and arbitrary porous structure in the study of squeeze step bearing lubricated with magnetic fluid considering variable magnetic field, *Journal of Engineering Tribology* 229(5) (2015) 646-659.

[54]   H. Christensen, Some aspects of the functional influence of surface roughness in lubrication, *Wear* 17 (1971) 149-162.

[55]   G.W. Stachowiak and A.W.Batchelor, *Engineering Tribology*, Butterworth Heinemann, London (2001).

[56]   J.R. Lin, Squeeze-film characteristics between a sphere and a flat plate: couple stress fluid model, *Computers and Structures* 75 (2000) 73-80.